

New Quasi-Landau Structure of Highly Excited Atoms: The Hydrogen Atom

J. Main, G. Wiebusch, A. Holle, and K. H. Welge

Fakultät für Physik, Universität Bielefeld, D-4800 Bielefeld 1, Federal Republic of Germany

(Received 21 July 1986)

A basically new structure of quasi-Landau resonances is discovered with the magnetized hydrogen atom around the ionization threshold. The resonances are theoretically rationalized by classical-trajectory calculation. In energy spacing and corresponding resonance time they form a highly regularly organized series with, classically, an infinite number of members.

PACS numbers: 31.60.+b, 32.60.+i

The physics of highly excited atoms around the ionization limit, that is, in the quasi-Landau (q-L) or strong-field-mixing regime¹ is still an unsolved fundamental problem of general importance,² with implications well beyond atomic physics.³ It is unsolved even for the H atom, that is, with the Hamiltonian in simplest form: $H = p^2/2 + \beta m + \beta^2 p^2/2 - 1/r$, where $\beta = B/(4.7 \times 10^5 \text{ T})$, in atomic units. Until recently, it had been generally accepted that the atomic q-L spectrum is governed by one resonance only, previously discovered by Garton and Tomkins.⁴ Characterized by the energy spacing $\Delta \epsilon_1 = \gamma_1 \hbar \omega_c$ ($\omega_c = eB/m_e$), the energy-dependent factor γ_1 of this resonance has a value, for instance, at the ionization limit ($E = 0$) of $\gamma_{10} = 1.5$. The resonance is explained by periodic two-dimensional motion of the electron perpendicular to the field in the $z = 0$ plane with period $T_{10} = 2\pi/\gamma_{10}\omega_c$.⁵

However, in first experiments with the H atom another new type of q-L resonance with $\gamma_{20} = 0.64$ has been recently observed, resulting from a three-dimensional motion of the excited electron out of the $z = 0$ plane.⁶ Though those experiments suggested the existence of even more resonances their structure and significance remained fully obscure. In this work we have discovered the resonances to form a series of strikingly simple and regular organization, not previously anticipated or predicted.

In principle, the same experimental technique as in the previous work has been employed, however, with the decisive difference of about five-times-higher spectral resolution. Balmer spectra of the H atom with final magnetic states $|m^f\rangle$ are excited in two steps with two (vuv+uv) pulsed tunable lasers: $H(1s, m^g=0) + \text{vuv light} \rightarrow H(2p, m^i) + \text{uv light} \rightarrow H(m^f)$. In the first step, pure Paschenack levels $|2p, m^i\rangle$ are prepared by tuning the vuv laser with appropriate polarization to individual transitions. From these levels, spectra have been taken at $B = 5.96 \text{ T}$ around the ionization limit in the range $-30 \text{ cm}^{-1} \leq E \leq +30 \text{ cm}^{-1}$ by scanning the uv laser. Figure 1 shows spectra of transitions $|2p, m^i=0\rangle \rightarrow |m^f=0\rangle$ and $|2p, m^i=-1\rangle \rightarrow |m^f=-1\rangle$. The zero point in the energy scale ($E = 0$) indicates the field-free ($B = 0$) ionization limit. The posi-

tions of energies marked by E_P and E_{IP} refer to the linear Zeeman shift $E_P = m^f \hbar e B / 2m_e$ and the Landau zero-point energy $E_{IP} = (m^f + |m^f| + 1) \cdot \hbar e B / 2m_e$. (Since spin and orbit are decoupled $|m^i = -1\rangle \rightarrow |m^f = -1\rangle$ and $|m^i = +1\rangle \rightarrow |m^f = +1\rangle$ transitions yield the same spectra, except for a corresponding linear shift in the energy scale.)

In contrast to the previous experiments, the present high-resolution spectra have lost virtually all regularity and show no q-L modulation. With their complex irregular structure of sharp lines they appear "chaotic." (It

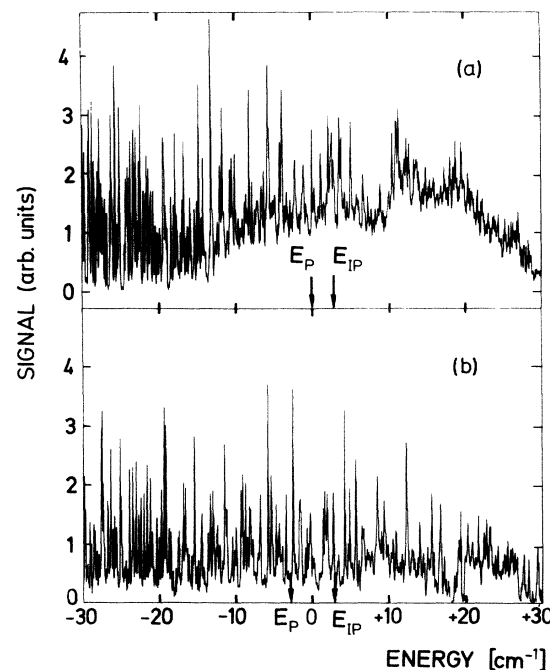


FIG. 1. Excitation ionization spectra of H-atom Balmer series around the ionization limit in a static homogeneous magnetic field. Field strength $B = 5.96 \text{ T}$; spectral resolution 0.07 cm^{-1} ; E_P , linear Zeeman shift; E_{IP} , Landau zero-point energy; $E = 0$, field-free ionization limit. (a) Initial state $|2p, m^i=0\rangle \rightarrow$ final state $|m^f=0\rangle$, even parity. (b) Initial state $|2p, m^i=-1\rangle \rightarrow$ final state $|m^f=-1\rangle$, even parity.

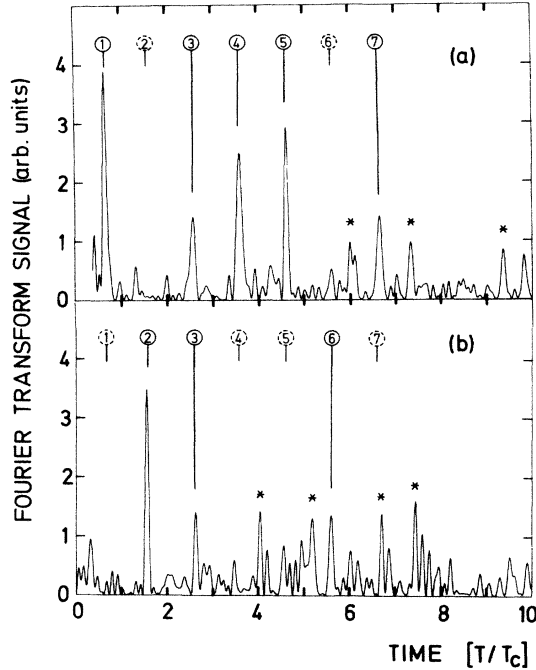


FIG. 2. Fourier-transformed spectra (a) and (b) in Fig. 1. Plotted is the absolute value squared. Abscissa with time scale normalized in units of T_c (see text).

should be noted that also in these spectra the resolution is still experimentally limited; the width of the narrowest lines is fully given by the uv-laser bandwidth.) Resonances are, however, more clearly exhibited in the time-domain Fourier-transformed spectra. They are plotted in Figs. 2(a) and 2(b) on a time scale normalized in terms of T/T_c , where $T_c = 2\pi/\omega_c = 6.0 \times 10^{-12}$ s is the cyclotron period. Clearly observable resonances are marked by integers, ν , in solid circles. Table I shows the experimental values of T_{ν}^{ex}/T_c and γ_{ν}^{ex} , related by $T_c/T_{\nu}^{\text{ex}} = \gamma_{\nu}^{\text{ex}}$. The ν -labeled resonances indicate a strikingly systematic organization: Except for the first ones, i.e., $\nu=1$ and $\nu=2$, nearest-neighbor resonances show, within experimental uncertainty ($\Delta T_{\nu}^{\text{ex}} \approx 0.05 T_c$), a practically constant spacing, $T_{\nu}^{\text{ex}} - T_{\nu-1}^{\text{ex}} = T_c$, i.e., just the cyclotron period. Positions of resonances not observed yet postulated from this relation are also indicated in the spectra (broken circles) and listed in Table I. The first few members evidently carry an essential fraction of the spectral oscillator strength. The resonances belonging to this ν series are called in the following "regular" or " ν type." The series can be rewritten in the form $T_{\nu}^{\text{ex}} = (\nu - \delta_{\nu}^{\text{ex}}) T_c$, where ν is a running integer and the quantities $\delta_{\nu}^{\text{ex}} \approx 0.3-0.4$ account for the defects from ν of each resonance. The known resonance ($\gamma_{10} = 1.5$) and the recently observed one ($\gamma_{20} = 0.64$) are recognized to be simply the first two members of this regular resonance family. Further resonances not fitting this sequence, however, clearly present in the Fourier spectra are marked by an asterisk. Their structure and nature

TABLE I. T_{ν}^{ex}/T_c : Experimental resonance times (T_{ν}^{ex}) normalized to cyclotron period $T_c = 6.0 \times 10^{-12}$ s at $B = 5.96$ T for final states $|m^f=0\rangle$ and $|m^f=-1\rangle$. T_{ν}^{th}/T_c : Normalized theoretical resonance time of the ν th trajectory at $E=0$. $\theta_{\nu 0}$: Starting angle of the ν th trajectory at $E=0$. $\Delta \epsilon_c = \hbar \omega_c$. $\Delta \epsilon_{\nu 0}$: Energy spacing of the ν th quasi-Landau resonance. $\delta_{\nu 0}$ given by $T_{\nu 0} = (\nu - \delta_{\nu 0}) T_c$.

ν	$\theta_{\nu 0}$ (deg)	$m^f=0$ T_{ν}^{ex}/T_c	$m^f=-1$ T_{ν}^{ex}/T_c	T_{ν}^{th}/T_c	$\gamma_{\nu 0} = \Delta \epsilon_{\nu 0}/\Delta \epsilon_c$	$\delta_{\nu 0}$
1	90.0	0.66	...	0.67	1.50	0.33
2	53.8	...	1.57	1.57	0.64	0.43
3	42.8	2.58	2.64	2.58	0.39	0.42
4	37.3	3.60	(3.49)	3.59	0.28	0.41
5	33.9	4.62	(4.57)	4.60	0.22	0.40
6	31.4	(5.60)	5.61	5.61	0.18	0.39
7	29.5	6.66	(6.73)	6.62	0.15	0.38

remains an open problem to be solved by more precise experiments.

The regular-type resonances can be physically rationalized and explained by *classical* periodic orbits of the electron on closed trajectories starting at and returning to the proton as origin with an orbital recurrence-time T characteristic for each ν -type resonance. This approach is in essence the classical approximation of the time-dependent wave-packet treatment previously applied by Reinhardt⁷ to the ($\nu=1$) resonance in the $z=0$ plane. As shown there, even a single return with recurrence time T of the wave packet suffices to produce a resonance with energy spacing $\Delta \epsilon = 2\pi\hbar/T$. The classical treatment is based generally on the WKB condition⁸ which is valid, except at the proton and turning points, to high degree, since the excited electron moves mostly in a space and potential of practically macroscopic dimensions. The breakdown of this classical approximation is indicated below.

As previously,⁶ trajectories are calculated, irrespective of the initially excited final-state orbital angular distribution, with the Hamiltonian (in cylindrical coordinates)

$$H = (p_{\rho}^2 + p_z^2 + p_{\phi}^2/\rho^2)/2 + \beta p_{\phi} + \beta^2 \rho^2/2 - (\rho^2 + z^2)^{-1/2}.$$

The ϕ motion can be separated off, i.e., the angular momentum p_{ϕ} is quantized with $p_{\phi} = m^f$, leaving the nonseparable (ρ, z) part. The special case of motion in the $z=0$ plane ($\theta=90^\circ$) can be solved for $m^f=0$ analytically,⁹ yielding specifically at $E=0$ the known q-L resonance with recurrence time $T_{10} = 2\pi/\gamma_{10}\omega_c$ ($\gamma_{10}=1.5$). Trajectories out of the $z=0$ plane are integrated numerically with initial conditions of ρ and z at time $t=0$ chosen as $\rho(t=0)=0$ and $z(t=0)=0$. This choice of initial conditions is physically suggestive since the electron is excited from the $2p$ state confined to within a few Bohr radii at the proton. The starting angle θ between the z axis and the initial velocity vector at the proton,

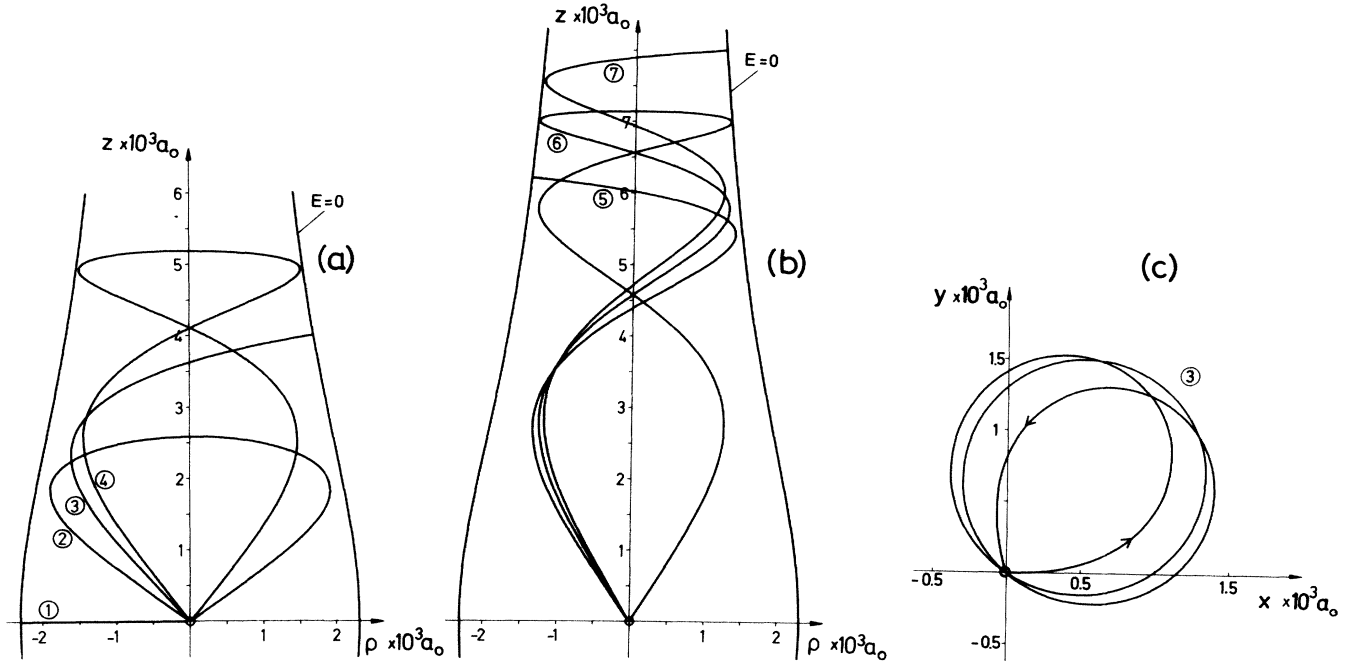


FIG. 3. (a),(b) Calculated closed trajectories of electron motion at energy $E=0$, corresponding to the first seven resonances $\nu=1, 2, \dots, 7$. Final state $|m^f=0\rangle$. Projection onto (ρ, z) coordinates. $E=0$: Potential of field-free ionization threshold. (c) Closed trajectory of $\nu=3$ type at $E=0$ in projection onto the $z=0$ plane. Final state $|m^f=0\rangle$.

and the excitation energy E are free parameters. We have performed calculations for states $m^f=0$ and 1 at various energies around the threshold and at angles between 0° to 90° . The distance from the origin at which the electron returns for the first time to the $z=0$ plane is a continuous function of θ and becomes zero at distinct angles $\theta_\nu(E)$, resulting in closed orbits with corresponding recurrence times $T_\nu(E)$.

First we present and discuss results of calculations at $E=0$. Figures 3(a) and 3(b) show the first seven trajectories ($\nu=1, \dots, 7$) for $m^f=0$ in projection onto the (ρ, z) coordinates. Figure 3(c) presents, as an example, the $\nu=3$ trajectory projected onto the $z=0$ plane. The $|m^f|=1$ trajectories are nearly the same as the $m^f=0$ ones, except close to the z axis where, as a result of the centrifugal barrier they pass closely around the z axis at a minimum distance given by $\rho_{\min} \approx |m^f|(|z|/2)^{1/2}$. ($z=0$ projections of the common $\nu=1^{10}$ and of the $\nu=2^6$ trajectories have been shown previously.) The calculated recurrence times $T_{\nu 0}$ (normalized again to T_c), the corresponding $\gamma_{\nu 0}$ factors, and defect quantities $\delta_{\nu 0}$ of the trajectories are given in Table I. They agree, within experimental precision, quantitatively with the experimentally observed ones, supporting the validity of the classical approximation and proving that the regular resonance series indeed is governed by the relation $T_{\nu 0} = (\nu - \delta_{\nu 0})T_c$. Conversion of the recurrence time to the energy spacing yields an equally simple relation $\Delta\epsilon_{\nu 0} = \Delta\epsilon_c / (\nu - \delta_{\nu 0})$, $\Delta\epsilon_c = \hbar\omega_c$. The resonances of this "regular" type thus form, classically, a series with an in-

finite number of members converging with $\nu \rightarrow \infty$ to $\Delta\epsilon_{\infty 0} = 0$. The defects $\delta_{\nu 0}$ vary systematically with ν , getting smaller with larger ν . Calculations for trajectories up to $\nu=30$ indicate that the defects converge to a limit $\delta_{\infty 0} \approx 0.3$. The regular behavior of the ν -type resonances has a simple physical reason: The orbits grow with ν by one additional cycle into the z direction where the motion becomes increasingly purely cyclotronlike with period T_c . The term $\delta_{\nu 0}T_c$ simply accounts for the action of the Coulomb field, the relative effect of which decreases with ν .

As to the energy dependence, trajectory calculations as a function of E reveal an unexpected general property of the ν -type resonances: Except for the known $\nu=1$ resonance for which trajectories exist at all positive and negative energies, all $\nu \geq 2$ trajectories are found to degenerate at distinct negative "cutoff" energies, $E = -|E_{\nu, \text{cut}}|$, to a linear motion exactly along the z axis, on which the potential is purely Coulombic. Depending on the field strength each resonance-type ν has a characteristic cutoff shifting systematically with ν to higher energies and converging with $\nu \rightarrow \infty$ to $E_{\infty, \text{cut}} = 0$. This behavior is illustrated in Fig. 4 by the $\nu=2$ type at $B=6$ T as an example. The trajectories are drawn at energies differing by constant increments of $\Delta E = 5 \text{ cm}^{-1}$. Obviously, the cutoff regime is where the classical treatment ceases to be applicable to the regular $\nu \geq 2$ resonances.

As to the intensity distribution of the resonances, it remains an unsolved problem. Some distinct features,

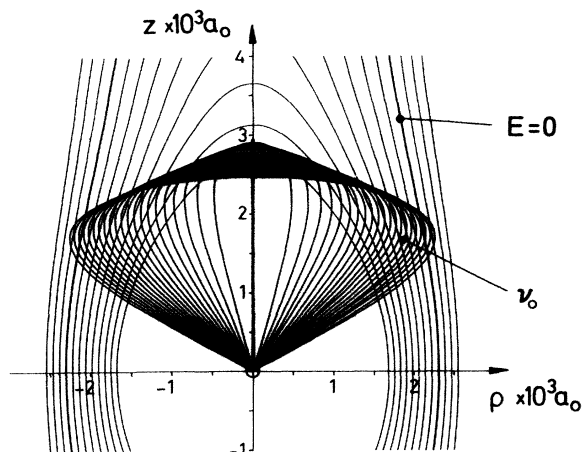


FIG. 4. Energy dependence of closed trajectories of $\nu=2$ type in (ρ, z) projection. Final state $|m^f=0\rangle$. Equidistant (10 cm^{-1}) potential lines. $E=0$: Field-free ionization potential. ν_0 : Trajectory at $E=0$. Trajectories drawn in energy increments of 5 cm^{-1} .

particularly the missing of the $\nu=2$ and $\nu=1$ resonances in the respective spectra of Figs. 2(a) and 2(b) can, however, be qualitatively rationalized on the basis of the time-dependent wave-packet model.⁷ There the intensity of a resonance will depend on the angular distribution of the final-state hydrogenic partial wave $Y_{lm}(\theta, \phi)$. In the $|d; m^f = -1\rangle$ spectrum $Y_{21}(\theta, \phi)$ has a node in the $z=0$ plane, i.e., just at the starting angle ($\theta_1=90^\circ$) of the $\nu=1$ trajectory. Similarly, the partial waves of $|s; m^f=0\rangle$ and $|d; m^f=0\rangle$ involved in the excitation of the $|m^f=0\rangle$ spectrum have relatively small amplitudes at the starting angle $\theta_{20}=53.8^\circ$ of the $\nu=2$ trajectory. The spherical harmonic $Y_{20}(\theta, \phi)$ has a node at $\cos\theta=1/\sqrt{3}$ ($\theta=54.7^\circ$) close to the $\nu=2$ starting angle and the amplitude of $Y_{00}(\theta, \phi)$ is altogether relatively small since the ratio of the total excitation cross sections of the s and d waves is 1:12.8.¹¹

In summary, a fundamentally new structure of q-L resonances organized systematically in a simple regular series with, classically, an infinite number of members has been discovered. The resonances are quantitatively accounted for by classical trajectory calculation revealing three-dimensional electron orbits of Lissajous form. Theoretical analysis of the energy dependence shows that the three-dimensional resonances degenerate, classically, at distinct negative cutoff energies to one-dimensional electron motion along the field axis, indicating the

breakdown of the applied classical approximation.

In conclusion, we wish to add that the classical approach presented can be straightforwardly extended to a semiclassical quantitative treatment by Einstein-Brillouin-Keller (EBK) calculation of multidimensional nonseparable systems.¹² After separation of the conserved ϕ motion, the three-dimensional trajectories are quantized by employing the Bohr-Sommerfeld condition generalized to two dimensions: $\oint_{(v)} (p_\rho d\rho + p_z dz) = 2\pi n_v \hbar$, where the quantum number n_v represents the number of nodes of standing de Broglie waves along the respective closed ν -type classical trajectories. Through the Hamiltonian n_v is a function of E and B . Numerical solution of the line integral for all ν -type trajectories with E and B as parameters yields the resonance spectrum $n_v(E, B)$, including, in particular, the most challenging regime around threshold where no exact quantum mechanical solution is known.

The work has been supported by a grant from Deutsche Forschungsgemeinschaft.

¹A. R. P. Rau, Phys. Rev. A **16**, 613 (1977).

²D. Kleppner, M. G. Littman, and M. L. Zimmerman, in *Rydberg States of Atoms and Molecules*, edited by R. F. Stebbings and F. B. Dunning (Cambridge Univ. Press, Cambridge, England, 1983), pp. 73-116.

³J. C. Gay, in *Progress in Atomic Spectroscopy, Part C*, edited by H. J. Beyer and H. Kleinpoppen (Plenum, New York, 1984), pp. 177-246.

⁴W. R. S. Garton and F. S. Tomkins, Astrophys. J. **158**, 839 (1969).

⁵A. F. Starace, J. Phys. B **6**, 585 (1973).

⁶A. Holle, G. Wiebusch, J. Main, B. Hager, H. Rottke, and K. H. Welge, Phys. Rev. Lett. **56**, 2594 (1986).

⁷W. P. Reinhardt, J. Phys. B **16**, L635 (1983).

⁸L. D. Landau and E. M. Lifshitz, *Quantum Mechanics* (Addison-Wesley, Reading, MA, 1965), 2nd ed., Sect. 46.

⁹J. A. C. Gallas and R. F. O'Connell, J. Phys. B **15**, L75 (1982).

¹⁰C. W. Clark, K. T. Lu, and A. F. Starace, in *Progress in Atomic Spectroscopy, Part C*, edited by H. J. Beyer, and H. Kleinpoppen (Plenum, New York, 1984), pp. 247-320.

¹¹H. A. Bethe, and E. E. Salpeter, *Quantum Mechanics of One- and Two-Electron Atoms* (Springer-Verlag, Berlin, Germany, 1957), 1st ed., Sect. 63.

¹²A. Einstein, Verh. Dtsch. Phys. Ges. (Berlin) **19**, 82 (1917); L. Brillouin, J. Phys. Radium **7**, 353 (1926); J. B. Keller, Ann. Phys. (N.Y.) **4**, 180 (1958); as a review see I. C. Percival, Adv. Chem. Phys. **36**, 1 (1977).

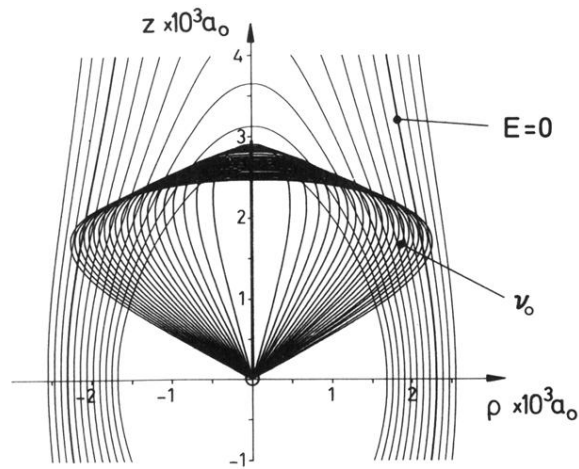


FIG. 4. Energy dependence of closed trajectories of $\nu=2$ type in (ρ, z) projection. Final state $|m^f=0\rangle$. Equidistant (10 cm^{-1}) potential lines. $E=0$: Field-free ionization potential. ν_0 : Trajectory at $E=0$. Trajectories drawn in energy increments of 5 cm^{-1} .